Am J Physiol Heart Circ Physiol 286: H195–H201, 2004.
First published August 28, 2003; 10.1152/ajpheart.00667.2003.

Internalization of caveolin-1 scaffolding domain facilitated by Antennapedia homeodomain attenuates PAF-induced increase in microvessel permeability

Longkun Zhu,[1] Diane Schwegler-Berry,[2] Vince Castranova,[2] and Pingnian He[1]

[1]*Department of Physiology and Pharmacology, West Virginia University, and* [2]*Pathology and Physiology Branch, Health Effects Laboratory Division, National Institute of Occupational Safety and Health, Morgantown, West Virginia 26506*

Submitted 14 July 2003; accepted in final form 25 August 2003

Zhu, Longkun, Diane Schwegler-Berry, Vince Castranova, and Pingnian He. Internalization of caveolin-1 scaffolding domain facilitated by Antennapedia homeodomain attenuates PAF-induced increase in microvessel permeability. *Am J Physiol Heart Circ Physiol* 286: H195–H201, 2004. First published August 28, 2003; 10.1152/ajpheart.00667.2003.—We demonstrated previously that inhibition of endothelial nitric oxide synthase (NOS), using pharmacological inhibitors, attenuated the ionomycin- and ATP-induced increases in microvessel permeability (*Am J Physiol Heart Circ Physiol* 272: H176–H185, 1997). Recently, the scaffolding domain of caveolin-1 (CAV) has been implicated as a negative regulator of endothelial NOS (eNOS). To examine the role of CAV-eNOS interaction in regulation of permeability in intact microvessels, the effect of internalized CAV on the platelet-activating factor (PAF)-induced permeability increase was investigated in rat mesenteric venular microvessels. Internalization of CAV was achieved by perfusion of individual vessels using a fusion peptide of CAV with Antennapedia homeodomain (AP-CAV) and visualized by fluorescence imaging and electron microscopy. Changes in microvessel permeability were evaluated by measuring hydraulic conductivity (L_p) in individually perfused microvessels. We found that the PAF (10 nM)-induced L_p increase was significantly attenuated from 6.0 ± 0.9 ($n = 7$) to 2.0 ± 0.3 ($n = 5$) times control after microvessels were perfused with 10 μM AP-CAV for 2 h. The magnitude of this reduction is comparable with that of the inhibitory effect of N^{ω}-monomethyl-L-arginine on the PAF-induced L_p increase. In contrast, perfusion with 10 μM AP alone for 2 h modified neither basal L_p nor the vessel response to PAF. These results indicate that CAV plays an important role in regulation of microvessel permeability. The inhibitory action of CAV on permeability increase might be attributed to its direct inactivation of eNOS. In addition, this study established a method for studying protein-protein interaction-induced functional changes in intact microvessels and demonstrated AP as an efficient vector for translocation of peptide across the cell membrane in vivo.

endothelial nitric oxide synthase; nitric oxide; caveolae; individually perfused venular microvessel; hydraulic conductivity

OUR LABORATORY AND SEVERAL other investigators, using pharmacological approaches, demonstrated that the increased nitric oxide (NO) production induced by inflammatory mediators is a necessary signaling pathway to increase microvessel permeability (11, 12, 17–20, 22, 26). Recently, it was reported that caveolin-1, the principal structural protein in the caveolae of endothelial cells, interacts with a wide variety of signaling molecules, and endothelial NO synthase (eNOS) is one of its well-characterized targets (7, 9, 16). It was demonstrated that caveolin-1 inhibits eNOS activity by a direct interaction with eNOS through its "scaffolding domain," located between amino acids 82 and 101 within endothelial plasmalemmal caveolae (15). A 16-amino acid peptide of *Drosophila* Antennapedia homeodomain (AP) can facilitate the translocation of caveolin-1 scaffolding domain (CAV) across the cell membrane and can reduce inflammation in vivo (1).

The objectives of our present study are as follows: *1*) to apply an AP-linked CAV to individually perfused microvessels to establish a method for the study of endothelial protein-protein interaction-induced functional changes in intact microvessels and *2*) to examine the effect of caveolin-1-eNOS interaction on microvessel permeability to further elucidate the role of NO in regulation of microvessel permeability. Delivery of CAV to microvessel endothelial cells was achieved by perfusing individual vessels using a fusion peptide of CAV with AP (AP-CAV). Changes in microvessel permeability were evaluated by measuring hydraulic conductivity (L_p) in rat mesenteric venular microvessels. The effect of internalized CAV on microvessel permeability was investigated before and after exposure of the same microvessel to platelet-activating factor (PAF). The effect of inhibition of NOS by pharmacological agents on PAF-induced permeability increase was also investigated. Such studies provide a parallel comparison with results obtained from application of AP-CAV. Internalization of CAV in endothelial cells forming microvessel walls was illustrated with fluorescence imaging and electron microscopy.

MATERIALS AND METHODS

Animal preparation. Experiments were carried out in venular microvessels in rat mesenteries. All procedures and animal use were approved by the Animal Care and Use Committees at West Virginia University. Female Sprague-Dawley rats (2–3 mo old, 220–250 g; Hilltop Laboratory Animal, Scottsdale, PA) were anesthetized with pentobarbital sodium given subcutaneously. The initial dose was 65 mg/kg body wt, and an additional 3 mg/dose was given as needed. The trachea was intubated, and a midline surgical incision (1.5–2 cm) was made in the abdominal wall. The rat was then transferred to a tray and kept warm on a heating pad. The mesentery was gently taken out from the abdominal cavity and spread over a pillar for measurement of L_p. The upper surface of the mesentery was superfused continuously with mammalian Ringer solution during preparation and experimentation. The temperature of the superfusate was maintained at 37°C and was monitored by a thermometer probe placed at the superfusate dripper and regulated by a digitally controlled water bath. All experiments were carried out in venular microvessels, which were classified as segments where there is convergent flow two to four branches distal to true capillaries. The mean diameter of all vessels

Address for reprint requests and other correspondence: P. He, Dept. of Physiology and Pharmacology, School of Medicine, Health Sciences Center North, West Virginia Univ., Morgantown, WV 26506-9229 (E-mail: phe@hsc.wvu.edu).

The costs of publication of this article were defrayed in part by the payment of page charges. The article must therefore be hereby marked "*advertisement*" in accordance with 18 U.S.C. Section 1734 solely to indicate this fact.

used for the experiments was 40 ± 8 (SD) μm (n = 36). Blood flow was brisk in all the vessels selected for experiments, and there was no more than one adherent leukocyte per 100 μm of vessel wall.

Measurement of L_p in single perfused rat mesenteric microvessels. All measurements were based on the modified Landis technique, which measures the volume flux of water across the microvessel wall (3). The assumptions and limitations of the original method and its application in mammalian microvessels have been evaluated in detail elsewhere (3, 14). Briefly, a single venular microvessel was cannulated with a glass micropipette and perfused with albumin-Ringer solution (control) containing 1% (vol/vol) rat red blood cells as markers. A hydrostatic pressure (range 50–80 cmH_2O) controlled by a water manometer was applied through the micropipette to the microvessel lumen. A charge-coupled device camera was connected to the microscope, and a video was recorded from a segment of the perfused microvessel (400 μm long) throughout each experiment for data analysis. The initial water flow per unit area of microvessel wall [$(J_v/S)_0$, where J_v is water flow and S is unit area of the microvessel wall] was calculated from the velocity of the marker cell after the vessel was occluded, the vessel radius, and the distance between the marker cell and the occlusion site. Any vessel diameter changes can be precisely measured from the video images, which are incorporated into the L_p calculation. To avoid the effect of vessel compliance on marker cell movement, velocity of the marker cell was calculated after 2 s of occlusion. Microvessel L_p was calculated from the Starling equation as follows: $L_p = (J_v/S)/\Delta P$, where ΔP is the effective hydrostatic and oncotic pressure difference across the microvessel wall. If the tissue hydrostatic and oncotic pressures are assumed to be negligible, ΔP represents the pressure difference between the hydrostatic pressure applied to the microvessel and the effective oncotic pressure generated from albumin in the perfusate (BSA at 10 mg/ml has effective oncotic pressure of 3.6 cmH_2O). In each experiment, control L_p was measured first with albumin-Ringer perfusate. Then multiple recannulations were made in the same vessel to measure changes in L_p in response to different testing agents. The mean L_p for each perfusate was calculated from all occlusions during that perfusion period, if L_p is relatively constant in the whole time course. Otherwise, L_p is reported as the means of peak and sustained values, if a transient increase in L_p is observed. To translocate peptide across endothelial membrane, each vessel was perfused with albumin-Ringer solution containing AP or AP-CAV (10 μM) for 2 h. Changes in L_p in response to the testing agent were measured in the presence of the loading peptide.

Fluorescence microscopy. Experiments were carried out with a Nikon 300 Diaphot inverted microscope. Each selected venular microvessel was cannulated and perfused with an albumin-Ringer solution containing 10 μM FITC-labeled AP (F-AP) or AP-CAV (F-AP-CAV) for 2 h in the dark at 37°C. After loading was completed, the vessel was recannulated and perfused with albumin-Ringer solution to wash out F-AP or F-AP-CAV from the vessel lumen. Fluorescence images were acquired by a Hamamatsu digital camera with a ×40 oil objective (NA 1.3) through a Nikon FITC HYQ filter set (excitation 480/40 nm, dichroic mirror 505 nm, and band-pass barrier 535/50 nm) and processed with Universal Imaging software.

Electron microscopy. Biotinylated AP-CAV (B-AP-CAV) was used for electron microscopy to visualize the distribution of internalized AP-CAV in the endothelial cells. Each individually cannulated microvessel was perfused with 10 μM B-AP-CAV in albumin-Ringer solution for 2 h and perfused with albumin-Ringer solution to wash out B-AP-CAV from the vessel lumen. The upper surface of the mesentery was then superfused with a fixative solution of paraformaldehyde (1%), glutaraldehyde (1.25%), and 5% sucrose in 0.1 M phosphate buffer (pH 7.4) for 20 min. After fixation, a small panel of mesentery containing the perfused microvessel was dissected out and allowed to sit in the same fixative at 4°C overnight. The selected tissue was then rinsed in 0.1 M phosphate buffer and permeabilized with 50% ethanol in H_2O. H_2O_2 (3%) was applied for 15 min to pretreat endogenous peroxidase before immunoperoxidase staining. The tissue was processed with the Vectastain Elite ABC kit (Vector Laboratories, Burlingame, CA) and reacted with diaminobenzidine. The tissues were to remain in ice at all steps. For the negative control, the fixation and immunostaining procedures described above were used, except the vessel was perfused with albumin-Ringer solution without B-AP-CAV. The samples were postfixed in osmium tetroxide (1%), dehydrated in a series of ethanol, transferred into propylene oxide, and embedded in Epon (Ladd LX112). Thin sections were stained with alcoholic uranyl acetate and Reynolds citrate. Micrographs (magnification ×32,400) were taken on a JEOL 1220 transmission electron microscope.

Solutions and reagents. Mammalian Ringer solution was used for dissecting mesenteries, superfusing tissue, and preparing the perfusion solutions. The composition of the mammalian Ringer solution was (in mM) 132 NaCl, 4.6 KCl, 2 $CaCl_2$, 1.2 $MgSO_4$, 5.5 glucose, 5.0 $NaHCO_3$, and 20 HEPES and Na-HEPES. The pH of the Ringer solution was maintained at 7.40–7.45 by adjusting the ratio of Na-HEPES to HEPES. All perfusates used for control and test perfusion contained BSA (10 mg/ml).

1-*O*-alky1–2-acetyl-*sn*-glycero-3-phosphocholine (PAF) and N^{ω}-monomethyl-L-arginine (L-NMMA) were purchased from Sigma. AP, the Antennapedia internalization sequence from *Drosophila* Antennapedia homeodomain (amino acids 43–58, RQIKIWFQNRRMKWKK), was purchased from CN Biosciences (San Diego, CA). AP-CAV, the fusion peptide of CAV (amino acids 82–101, DGIWKASFTTETVTKYWFYR) with AP, was custom synthesized by Tufts University with sequences identical to that published by Bucci et al. (1). Biotin- or FITC-labeled peptides (B-AP-CAV, F-AP, and F-AP-CAV) were synthesized by conjugation of identical biotin or FITC to the NH_2 terminus of AP or AP-CAV, respectively. Stock solutions of each peptide (10 mM) were prepared with 100% DMSO. The final concentration of each peptide, 10 μM, was achieved by 1:1,000 dilution of the stock with albumin-Ringer solution. PAF was initially dissolved in 95% ethyl alcohol (5 mM) and further diluted to a final concentration of 10 nM with albumin-Ringer solution. All perfusates were freshly prepared with albumin-Ringer solution before each cannulation.

Data analysis and statistics. Values are means ± SE, except where noted otherwise. Changes in L_p are expressed as the ratio of testing L_p to control L_p. The mean values of L_p (control and test) measured in the same vessel were used as paired data. The significance of the differences within or between groups was evaluated by paired t-test and analysis of variance. $P < 0.05$ was considered statistically significant.

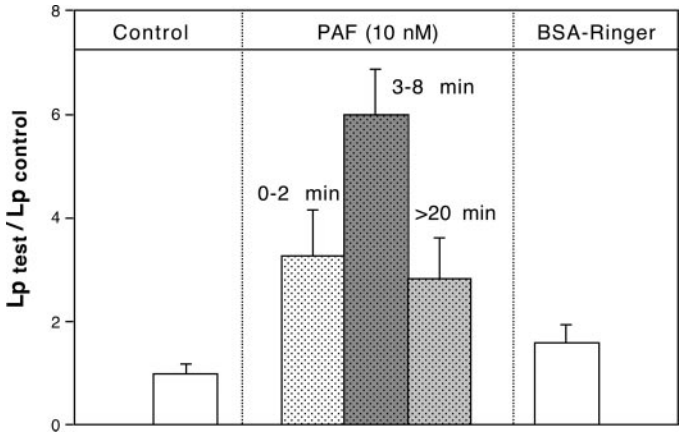

Fig. 1. Transient increases in hydraulic conductivity (L_p) after each vessel was exposed to 10 nM platelet-activating factor (PAF). $L_{ptest}/L_{pcontrol}$, ratio of testing to control L_p. Values are means ± SE (n = 7).

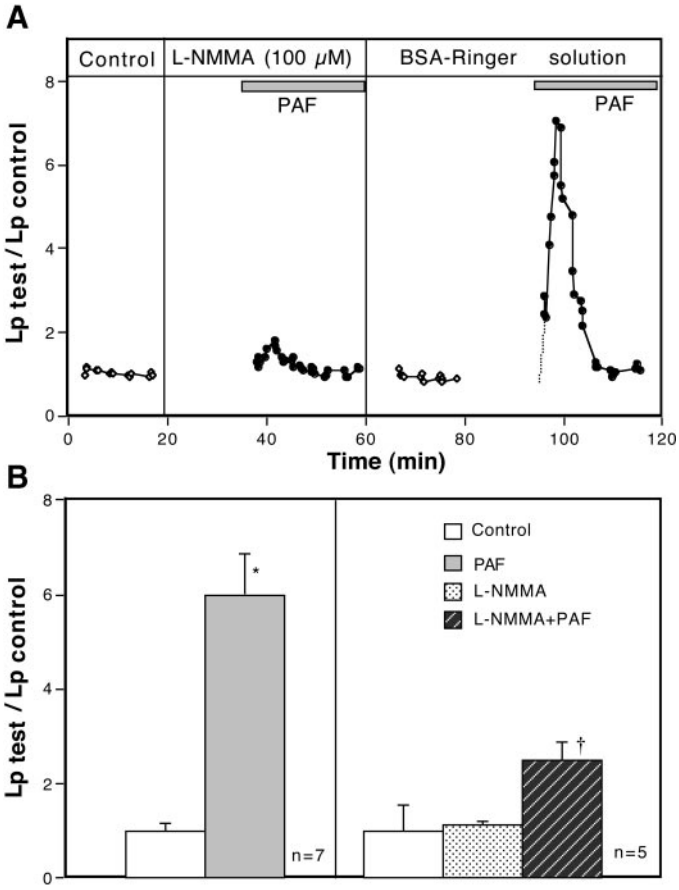

Fig. 2. Effect of the nitric oxide synthase (NOS) inhibitor N^{ω}-monomethyl-L-arginine (L-NMMA) on PAF-induced increases in microvessel permeability. *A*: paired measurements of L_p in response to 10 nM PAF with and without 100 μM L-NMMA in a single vessel. Control L_p was $1.4 \pm 0.1 \times 10^{-7}$ $cm \cdot s^{-1} \cdot cmH_2O^{-1}$. After the vessel was perfused with L-NMMA for 15 min, the peak increase in L_p in response to 10 nM PAF was only 1.5 times control. After washout of L-NMMA from the vessel lumen for 30 min, the PAF-induced peak increase in L_p recovered to 6.6 times control. *B*: PAF-induced mean peak increases in L_p with and without L-NMMA. Values are means ± SE. *Significant increase from negative control; †significant decrease from positive control.

RESULTS

Effect of PAF on microvessel L_p. The effect of 10 nM PAF on microvessel L_p was examined in seven microvessels. The mean control L_p measured with albumin-Ringer perfusate was $2.7 \pm 0.5 \times 10^{-7}$ $cm \cdot s^{-1} \cdot cmH_2O^{-1}$. L_p was transiently increased when each vessel was perfused with albumin-Ringer solution containing 10 nM PAF. The mean peak increase in L_p was 6.0 ± 0.9 times the control value, which occurred during 3–8 min of the PAF exposure. The increased L_p fell to 2.8 ± 0.8 times that of the control after 20 min of exposure to PAF. Results are summarized in Fig. 1.

L-NMMA attenuates PAF-induced L_p increase. To investigate the role of NO in the PAF-induced L_p increase, L-NMMA, an NOS inhibitor, was applied to the vessel lumen before PAF exposure. The mean control L_p of five vessels was $2.2 \pm 0.8 \times 10^{-7}$ $cm \cdot s^{-1} \cdot cmH_2O^{-1}$. After each vessel was perfused with solution containing 100 μM L-NMMA for 10 min, the mean L_p was $2.3 \pm 0.7 \times 10^{-7}$ $cm \cdot s^{-1} \cdot cmH_2O^{-1}$, which was not significantly different from that of the control. Then each vessel was exposed to 10 nM PAF in the presence of L-NMMA. The mean peak increase in L_p was significantly reduced from 6.0 ± 0.9 (PAF alone) to 2.5 ± 0.4 times that of the control ($P < 0.01$). The reversibility of the effect of L-NMMA on the PAF response was examined in two of the five microvessels. The PAF-induced peak increase in L_p recovered to 6.5 ± 0.2 times the control value after 30 min of perfusion with albumin-Ringer solution to wash out the previous agents from the vessel lumen. Figure 2*A* shows the time course and magnitude changes in L_p from one of the experiments. Figure 2*B* shows the comparison of the mean PAF responses with and without L-NMMA.

Effect of internalization of AP on basal L_p and PAF-induced L_p increase. It was reported that a 16-amino acid peptide corresponding to the third helix of AP is internalized by cells in culture (4). This peptide has been used to facilitate translocation of CAV across cell membranes systemically or in aortic rings (1). Before investigating the effect of uptake of AP-CAV on microvessel permeability in individually perfused microvessels, we examined the effects of internalization of AP alone on basal L_p and the microvessel responses to PAF. The mean control L_p measured in five microvessels was $1.8 \pm 0.2 \times 10^{-7}$ $cm \cdot s^{-1} \cdot cmH_2O^{-1}$. After 2 h of perfusion with 10 μM AP, the mean L_p was $1.7 \pm 0.4 \times 10^{-7}$ $cm \cdot s^{-1} \cdot cmH_2O^{-1}$. Then each vessel was exposed to 10 nM PAF in the presence of AP. The mean ratio of the peak L_p increase to that measured before the addition of PAF was 6.2 ± 0.8, which was not significantly different from the mean peak L_p increase measured with PAF alone. These results demonstrated that the uptake of AP modified neither basal L_p nor the vessel responses to PAF. Figure 3 shows the time course of the L_p changes in one of the experiments.

Internalization of CAV to endothelial cells attenuates PAF-induced increase in microvessel L_p. The role of CAV in PAF-induced increases in microvessel permeability was examined in five microvessels. After control L_p was measured, each vessel was perfused with 10 μM AP-CAV for 2 h to translocate CAV into endothelial cells forming microvessel walls. Perfusion of 10 μM AP-CAV for 2 h did not significantly change the

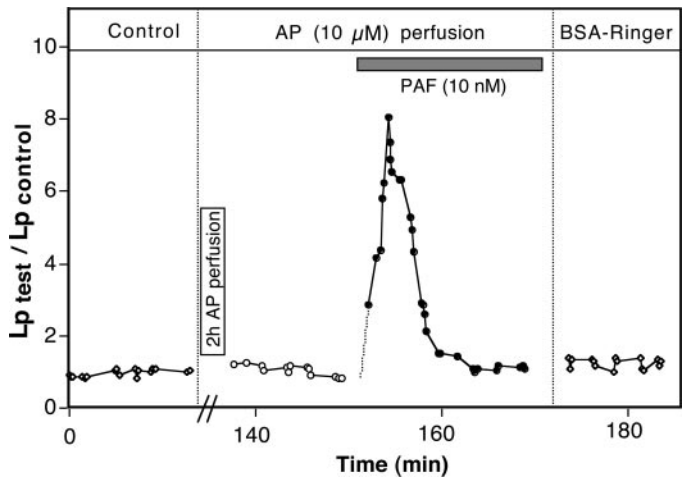

Fig. 3. Effect of internalization of Antennapedia homeodomain (AP) on basal L_p and PAF-induced L_p increase. Results from a single experiment show that internalization of AP did not modify basal L_p or magnitude and time course of the L_p increase in response to 10 nM PAF.

baseline L_p (2.0 ± 0.5 vs. $2.1 \pm 0.4 \times 10^{-7}$ cm·s^{-1}·cmH_2O^{-1}) but significantly attenuated the PAF response. The mean peak increase in L_p in response to PAF was reduced to 2.0 ± 0.3 times the control, measured after AP-CAV perfusion. The magnitude of this reduction is comparable with the inhibitory effect of L-NMMA on PAF-induced L_p increase. Figure 4 shows the time course of the L_p changes in a single experiment. Figure 5*A* shows the comparison of the mean time courses of PAF-induced L_p increases with internalization of AP and AP-CAV. Figure 5*B* compares the magnitude of PAF-induced peak L_p increases with those measured after application of L-NMMA, AP, or AP-CAV. The PAF-induced L_p increase was not significantly changed after AP perfusion but was significantly attenuated in L-NMMA- or AP-CAV-treated vessels.

We also examined the effect of 2 μM AP-CAV perfusion on the PAF-induced L_p increase. Perfusing vessels with 2 μM AP-CAV for 2 h did not significantly inhibit the PAF-induced L_p increase. The peak increase in L_p was 4.3 ± 1.5 times the control value ($n = 3$). A significant inhibition of PAF-induced L_p increase (2.4 ± 0.4 times control) was achieved by extending the perfusion time to 4 h ($n = 5$). To avoid the extended perfusion time in an intact microvessel, a 2-h perfusion with 10 μM AP-CAV was used as the optimum combination of peptide concentration and perfusion period for this study.

Uptake of AP and AP-CAV by endothelial cells forming microvessel walls. Uptake of AP and AP-CAV by endothelial cells in intact microvessels was visualized with fluorescence microscopy using F-AP and F-AP-CAV. Localization of the internalized AP-CAV was illustrated with electron microscopy using B-AP-CAV. Uptake of F-AP and F-AP-CAV was examined in eight microvessels (4 vessels for each peptide). Figure 6 shows representative fluorescence images after vessels were loaded with F-AP or F-AP-CAV. F-AP and F-AP-CAV were taken up by all endothelial cells of the perfused microvessel. In F-AP-loaded vessels, fluorescence was distributed throughout the endothelial cells, which yield a diffuse staining pattern (Fig. 6*A*). In contrast to the diffuse pattern of F-AP-loaded vessels, punctate distribution of fluorescence was observed in endothelial cells with F-AP-CAV-loaded microvessels, which was clearly illustrated when the focal plane was at the bottom

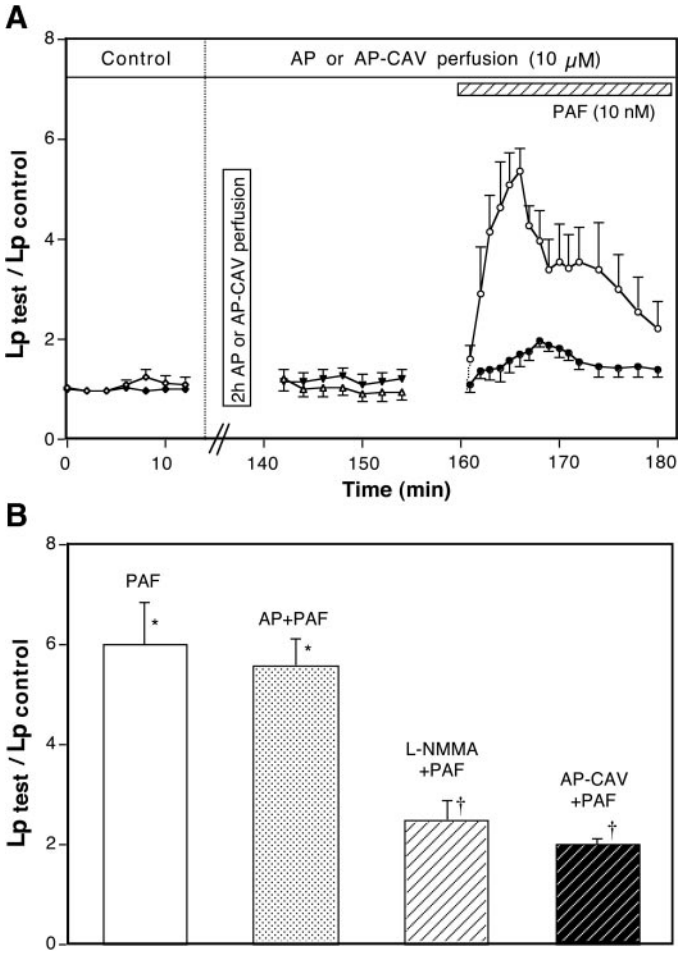

Fig. 5. Effects of uptake of AP alone and uptake of AP-CAV on basal L_p and PAF-induced L_p increase. *A*: mean values of $L_{ptest}/L_{pcontrol}$ with uptake of AP alone (open symbols, $n = 5$) and AP-CAV (filled symbols, $n = 5$) plotted as a function of time. *B*: magnitudes of mean peak increases in L_p in response to PAF under control conditions [i.e., normal Ringer perfusion (PAF, $n = 7$)], after internalization of AP (AP + PAF, $n = 5$), after perfusion of L-NMMA (L-NMMA + PAF, $n = 5$), and after internalization of AP-CAV (AP-CAV + PAF, $n = 5$). *Significant increase from negative control; †significant decrease from positive control.

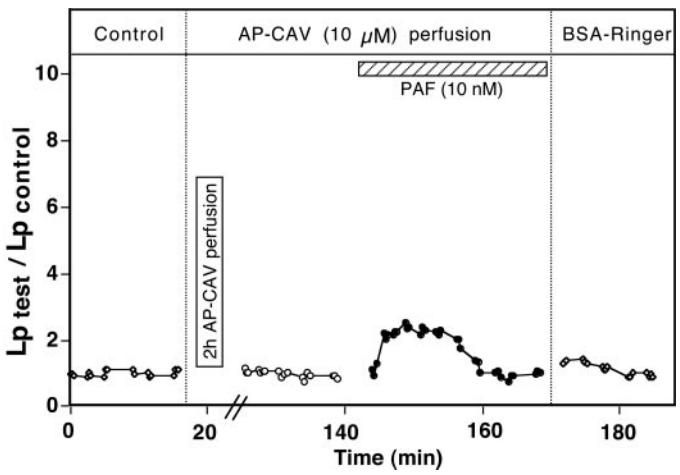

Fig. 4. Results from a single experiment showing that AP-facilitated scaffolding domain of caveolin-1 (AP-CAV) internalization did not change basal L_p but significantly attenuated PAF-induced L_p increase.

of the endothelial cell layer of the vessel wall (Fig. 6*B*). These fluorescent spots appear to correlate with the pattern of the caveolar invaginations shown on the endothelial plasma membrane by scanning electron microscopy (21). Figure 7*A* shows the distribution of B-AP-CAV in endothelial cells of the microvessel wall. The darker spots coating the caveolae indicate that AP-CAV was mainly localized in endothelial caveolae of the microvessel walls. The control micrograph (Fig. 7*B*) was obtained with albumin-Ringer perfusion but was subjected to the same developing procedures used for B-AP-CAV perfusion. Three vessels of each group were studied for electron microscopy.

DISCUSSION

Two important findings of this study are as follows. First, we established a new effective approach for the study of protein-protein interaction in vivo using individually perfused intact microvessels. Our results demonstrated that the translocating properties of AP efficiently facilitate the transport of CAV

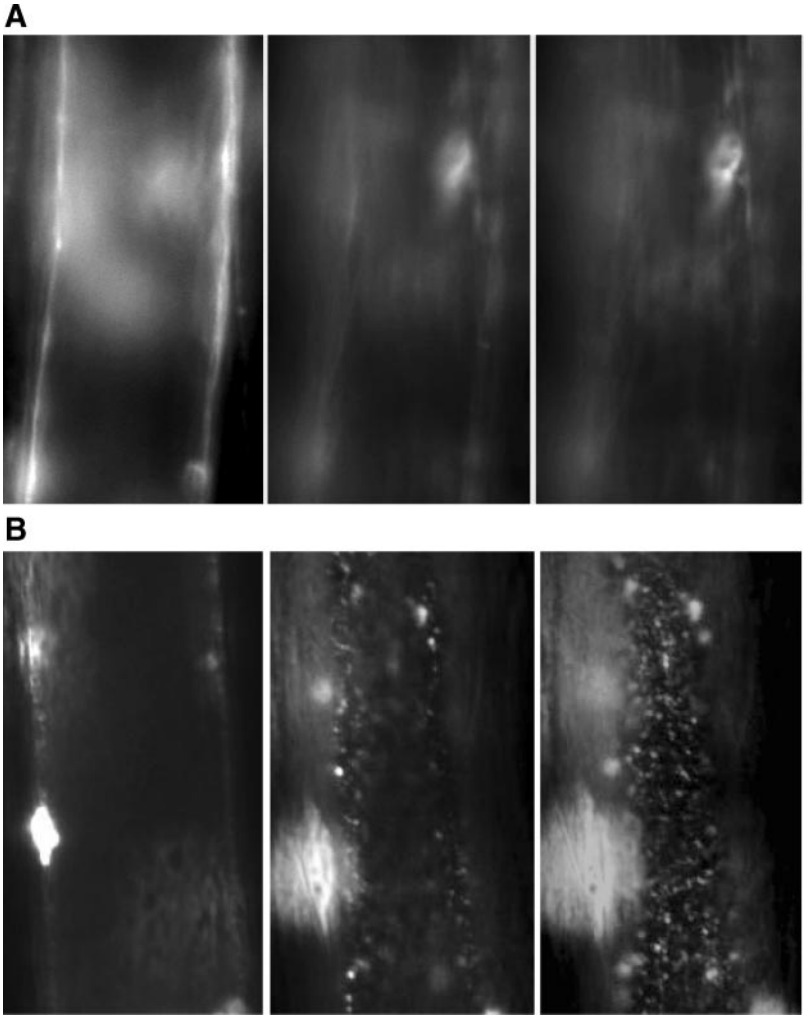

Fig. 6. Fluorescent images showing internalization of FITC-labeled AP (10 μM, *A*) and AP-CAV (10 μM, *B*) in individually perfused microvessels. Each set of images (from *left* to *right*) was taken at 3 different focal planes of the vessel (middle, lower quarter, and bottom, respectively). Spotted intracellular distribution of AP-CAV in endothelial cells forming microvessel walls is shown in *B*.

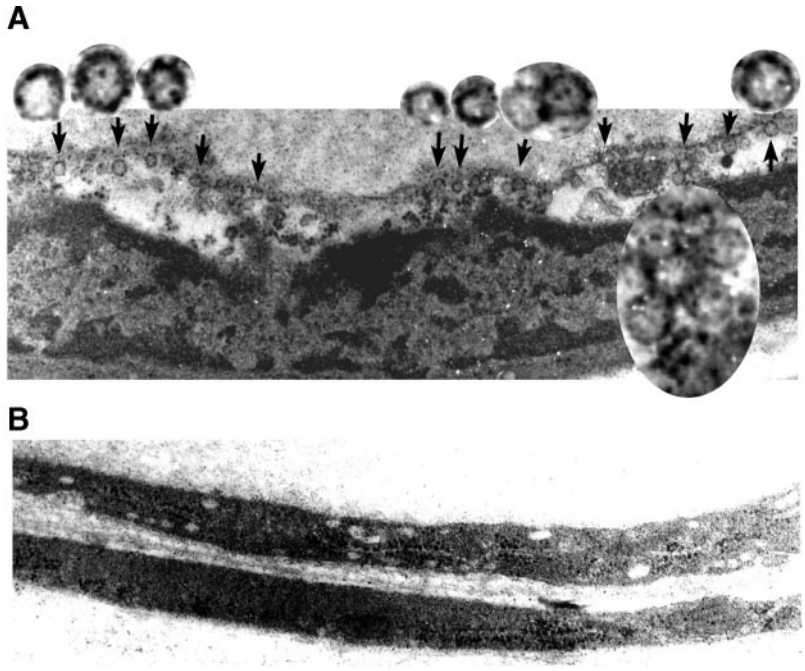

Fig. 7. Electron micrographs demonstrating colocalization of CAV with endothelial caveolae in microvessel wall. Thin cross sections were obtained from microvessels after perfusion with albumin-Ringer solution in the presence (*A*) or absence (*B*) of biotinylated AP-CAV (B-AP-CAV). Internalized B-AP-CAV, shown as darker spots, was preferentially accumulated in endothelial caveolae (*A*, arrows) after the vessel was perfused with B-AP-CAV for 2 h. *Insets*: B-AP-CAV-coated caveolae at a 3-times-higher magnification. *Large inset*: caveolae in clusters attached to endothelial plasma membrane containing B-AP-CAV peptides.

across the endothelial membrane after perfusion of AP-CAV in individually cannulated intact microvessels. More importantly, our results quantitatively demonstrated that internalization of AP alone does not modify basal L_p or the responses of microvessel permeability to inflammatory stimuli. Second, our results showed that internalization of AP-CAV significantly attenuates PAF-induced increases in microvessel permeability. The inhibitory action of AP-CAV is similar to that observed with the use of the NOS inhibitor L-NMMA. These results are consistent with the role of CAV, reported by several studies, as a negative regulator of eNOS in endothelial cells (1, 7, 8, 10, 13). This study provided further evidence to support our previous findings that the inflammatory mediator-induced NO release is a necessary step to increase microvessel permeability (11, 12). The NO-dependent pathway accounts for 70–80% of the PAF-induced L_p increase. The remaining increase may be attributed to other signaling pathways or mechanisms.

AP is an efficient vector for translocation of a biologically active compound across the endothelial cell membrane in individually perfused microvessels. The 16-amino acid polypeptide corresponding to the third helix of AP is able to transport polypeptides and oligonucleotides across biological membranes in cultured cells (5, 24). The internalization process appears to be mediated through direct interaction of AP with membrane phospholipids, which is receptor independent and nonendocytotic (4, 5). Recently, Bucci et al. (1) demonstrated that incubation of mouse aortic rings with 10 μM AP-CAV for 20 h inhibited acetylcholine-induced vasodilation and NO production. In addition, in vivo intraperitoneal delivery of AP-CAV reduced hindpaw and ear inflammation caused by local carrageenan injection and mustard oil application in mice (1).

Our fluorescence images (Fig. 6) demonstrated that, under our experimental conditions, perfusion for 2 h with albumin-Ringer solution containing 10 μM AP-CAV effectively translocates AP-CAV into endothelial cells in the intact microvessel wall, which is sufficient to attenuate the PAF-induced L_p increase. In most of the in vitro studies, the fluorescence-labeled CAV was loaded throughout the endothelial cells without a specific binding location (1). This is the first image that shows the spotted intracellular distribution of CAV in a live vessel using fluorescence microscopy, which is very well correlated with the pattern shown in caveolar invaginations on endothelial plasma membrane by scanning electron microscopy (21). In addition, B-AP-CAV (Fig. 7*A*) demonstrated the colocalization of caveolin-1 with caveolae in endothelial cells forming the microvessel wall. These results demonstrated that AP is an efficient vector to translocate a biologically active compound across the cell membrane. Compared with the techniques from other in vivo and in vitro studies, application of AP-facilitated internalization of peptide to individually perfused microvessels has some unique features. First, the single-vessel perfusion technique allows the solution containing peptide to have direct contact with endothelial cells lining the intact microvessel walls, which makes uptake of the peptide very efficient. Second, this technique enables repeated cannulation in the same vessel, so that basal L_p can be measured before and after uptake of each control or fusion peptide. Additionally, changes in permeability in response to inflammatory stimuli can be compared with control values measured in the same vessel, which minimizes the discrepancies between individual vessels and animals. Furthermore, microvessel permeability was measured at a known perfusion pressure, and the surface area for water and solute exchange can also be measured precisely. This is important for this particular study, because it enables us to distinguish the changes in microvessel permeability from the volume changes caused by changing flow dynamics and surface area due to eNOS inactivation and NO reduction. Reduced NO production would also promote leukocyte-endothelium interaction in the presence of blood components. Our experiments, conducted in the absence of blood elements, enable the role of internalization of caveolin-1 in the regulation of microvessel permeability to be studied independently from the permeability changes caused by the reduction of NO-induced leukocyte-endothelium interactions.

Internalization of CAV inhibits PAF-induced L_p increase: role of eNOS inactivation. Our previous study demonstrates that NOS inhibitors attenuated the permeability increases induced by ATP, bradykinin, and ionomycin in mesenteric venular microvessels (11, 12). Similar results have been reported for vascular endothelial growth factor-, histamine-, leukotriene C_4-, and PAF-induced permeability increases in different types of vessels and animal species (17, 18, 20, 22, 26). Increased NO production has been detected in cultured endothelial cells and in intact vasculature with bradykinin and PAF stimulation (2, 6). Our present study, showing the inhibition of PAF-induced L_p increase by L-NMMA in rat mesenteric venular microvessels, is further evidence supporting the hypothesis that increased NO production is a necessary signaling pathway resulting in increased microvessel permeability. However, because of the nonspecificity of NOS inhibitors used in previous studies, one cannot distinguish the type of NOS that is activated during stimulation and is responsible for the increased NO production.

Several in vitro and in vivo studies demonstrate that eNOS is markedly enriched in caveolae, where it colocalizes with caveolin-1, the primary structural coat protein of caveolae, suggesting a direct interaction between these two proteins (7, 9, 10). Functional studies show that caveolin-1, through binding its scaffolding domain to eNOS, inhibits eNOS activity in a dose-dependent manner (1, 9, 13). In caveolin-1-null animals, eNOS activity is upregulated because of the loss of caveolin-1 inhibition (23). These studies indicated that caveolin-1 is an endogenous inhibitor of eNOS.

As we demonstrated in this study, internalization of AP-CAV significantly attenuated the PAF-induced L_p increase, which indicated that caveolin-1 plays an important role in regulation of microvessel permeability under inflammatory conditions. Exogenous application of CAV in vivo may have the therapeutic potential to prevent the permeability increase during acute inflammation. A recent study by Duran et al. (6) showed an increase in NO production in the superfusate samples after hamster cheek pouch was exposed to PAF. A direct measurement of NO showed a reduction with AP-CAV internalization in cultured endothelial cells (1). In addition, the colocalization of eNOS and CAV has been reported by several investigators (8–10, 13). On the basis of these in vitro and in vivo studies, it is reasonable to speculate that NO is the potential key signaling molecule that contributes to the PAF-induced permeability increases and that the reduction of NO resulting from inhibition of eNOS by the internalized CAV is the mechanism accounting for attenuation of the PAF-induced

permeability increase. Because NOS inhibition has shown the inhibitory effect of permeability increases induced by a variety of stimuli (11, 12, 17–20, 22, 26), it is unlikely that the increased NO is unique for PAF exposure or for a specific stimulus. The increased eNOS activity might be a common reaction to inflammatory stimuli, and the activated eNOS-produced excessive NO is a key molecule leading to the increase in microvessel permeability.

Although evidence supports the hypothesis that the CAV-eNOS interaction is the mechanism attributed to the inhibitory action of CAV on the PAF-induced permeability increase, we recognize that CAV can potentially regulate a variety of signal transduction pathways in caveolae. Caveolin was also found in complexes with β_1-integrins and may be potentially linked to integrin function (25). We do not exclude the potential role of caveolin-1-integrin interaction in regulation of focal adhesion and microvessel permeability. Further in vivo and in vitro studies are needed to explore this possibility.

Summary. Internalization of a fusion peptide with AP provides a powerful tool for studying cellular protein-protein interaction-induced functional changes in intact microvessels. This study further demonstrated that the stimulated eNOS-derived excessive NO is the common signaling pathway for inflammatory mediator-induced increases in microvessel permeability. Furthermore, application of CAV has a significant inhibitory effect on the permeability increase during acute inflammation.

ACKNOWLEDGMENTS

We thank Dr. Alan R. Light for providing us electron microscopy protocol, Dr. Roger Adamson and Grete Adamson for comments on the electron micrographs, and Dr. Jun Liu for the AP-CAV used for some of the pilot experiments.

Some of the preliminary results were published as an abstract (27).

GRANTS

This study was supported by National Heart, Lung, and Blood Institute Grant HL-56237.

REFERENCES

1. **Bucci M, Gratton JP, Rudic RD, Acevedo L, Roviezzo F, Cirino G, and Sessa WC.** In vivo delivery of the caveolin-1 scaffolding domain inhibits nitric oxide synthesis and reduces inflammation. *Nat Med* 6: 1362–1367, 2000.
2. **Buckley BJ, Mirza Z, and Whorton AR.** Regulation of Ca^{2+}-dependent nitric oxide synthase in bovine aortic endothelial cells. *Am J Physiol Cell Physiol* 269: C757–C765, 1995.
3. **Curry PE, Huxley VH, and Sarelius IH.** Techniques in microcirculation: measurement of permeability, pressure and flow. In: *Cardiovascular Physiology. Techniques in the Life Sciences*. New York: Elsevier, 1983, p. 1–34.
4. **Derossi D, Calvet S, Trembleau A, Brunissen A, Chassaing G, and Prochiantz A.** Cell internalization of the third helix of the Antennapedia homeodomain is receptor-independent. *J Biol Chem* 271: 18188–18193, 1996.
5. **Derossi D, Joliot AH, Chassaing G, and Prochiantz A.** The third helix of the Antennapedia homeodomain translocates through biological membranes. *J Biol Chem* 269: 10444–10450, 1994.
6. **Duran WN, Seyama A, Yoshimura K, Gonzalez DR, Jara PI, Figueroa XF, and Boric MP.** Stimulation of NO production and of eNOS phosphorylation in the microcirculation in vivo. *Microvasc Res* 60: 104–111, 2000.
7. **Feron O, Belhassen L, Kobzik L, Smith TW, Kelly RA, and Michel T.** Endothelial nitric oxide synthase targeting to caveolae. Specific interactions with caveolin isoforms in cardiac myocytes and endothelial cells. *J Biol Chem* 271: 22810–22814, 1996.
8. **Garcia-Cardena G, Fan R, Stern DF, Liu J, and Sessa WC.** Endothelial nitric oxide synthase is regulated by tyrosine phosphorylation and interacts with caveolin-1. *J Biol Chem* 271: 27237–27240, 1996.
9. **Garcia-Cardena G, Martasek P, Masters BS, Skidd PM, Couet J, Li S, Lisanti MP, and Sessa WC.** Dissecting the interaction between nitric oxide synthase (NOS) and caveolin. Functional significance of the NOS caveolin binding domain in vivo. *J Biol Chem* 272: 25437–25440, 1997.
10. **Ghosh S, Gachhui R, Crooks C, Wu C, Lisanti MP, and Stuehr DJ.** Interaction between caveolin-1 and the reductase domain of endothelial nitric-oxide synthase. Consequences for catalysis. *J Biol Chem* 273: 22267–22271, 1998.
11. **He P, Liu B, and Curry FE.** Effect of nitric oxide synthase inhibitors on endothelial $[Ca^{2+}]_i$ and microvessel permeability. *Am J Physiol Heart Circ Physiol* 272: H176–H185, 1997.
12. **He P, Zeng M, and Curry FE.** cGMP modulates basal and activated microvessel permeability independently of $[Ca^{2+}]_i$. *Am J Physiol Heart Circ Physiol* 274: H1865–H1874, 1998.
13. **Ju H, Zou R, Venema VJ, and Venema RC.** Direct interaction of endothelial nitric oxide synthase and caveolin-1 inhibits synthase activity. *J Biol Chem* 272: 18522–18525, 1997.
14. **Kendall S and Michel CC.** The measurement of permeability in single rat venules using the red cell microperfusion technique. *Exp Physiol* 80: 359–372, 1995.
15. **Li S, Couet J, and Lisanti MP.** Src tyrosine kinases, Gα subunits, and h-Ras share a common membrane-anchored scaffolding protein, caveolin. Caveolin binding negatively regulates the auto-activation of Src tyrosine kinases. *J Biol Chem* 271: 29182–29190, 1996.
16. **Liu J, Garcia-Cardena G, and Sessa WC.** Palmitoylation of endothelial nitric oxide synthase is necessary for optimal stimulated release of nitric oxide: implications for caveolae localization. *Biochemistry* 35: 13277–13281, 1996.
17. **Mayhan WG.** Nitric oxide accounts for histamine-induced increases in macromolecular extravasation. *Am J Physiol Heart Circ Physiol* 266: H2369–H2373, 1994.
18. **Mayhan WG.** Role of nitric oxide in leukotriene C_4-induced increases in microvascular transport. *Am J Physiol Heart Circ Physiol* 265: H409–H414, 1993.
19. **Mayhan WG.** Role of nitric oxide in modulating permeability of hamster cheek pouch in response to adenosine 5′-diphosphate and bradykinin. *Inflammation* 16: 295–305, 1992.
20. **Mayhan WG.** VEGF increases permeability of the blood-brain barrier via a nitric oxide synthase/cGMP-dependent pathway. *Am J Physiol Cell Physiol* 276: C1148–C1153, 1999.
21. **Peters KR, Carley WW, and Palade GE.** Endothelial plasmalemmal vesicles have a characteristic striped bipolar surface structure. *J Cell Biol* 101: 2233–2238, 1985.
22. **Ramirez MM, Quardt SM, Kim D, Oshiro H, Minnicozzi M, and Duran WN.** Platelet-activating factor modulates microvascular permeability through nitric oxide synthesis. *Microvasc Res* 50: 223–234, 1995.
23. **Razani B, Engelman JA, Wang XB, Schubert W, Zhang XL, Marks CB, Macaluso F, Russell RG, Li M, Pestell RG, Di Vizio D, Hou H Jr, Kneitz B, Lagaud G, Christ GJ, Edelmann W, and Lisanti MP.** Caveolin-1-null mice are viable but show evidence of hyperproliferative and vascular abnormalities. *J Biol Chem* 276: 38121–38138, 2001.
24. **Theodore L, Derossi D, Chassaing G, Llirbat B, Kubes M, Jordan P, Chneiweiss H, Godement P, and Prochiantz A.** Intraneuronal delivery of protein kinase C pseudosubstrate leads to growth cone collapse. *J Neurosci* 15: 7158–7167, 1995.
25. **Wei Y, Yang X, Liu Q, Wilkins JA, and Chapman HA.** A role for caveolin and the urokinase receptor in integrin-mediated adhesion and signaling. *J Cell Biol* 144: 1285–1294, 1999.
26. **Wu HM, Huang Q, Yuan Y, and Granger HJ.** VEGF induces NO-dependent hyperpermeability in coronary venules. *Am J Physiol Heart Circ Physiol* 271: H2735–H2739, 1996.
27. **Zhu L and He P.** In vivo delivery of caveolin-1 scaffolding domain attenuates PAF-induced increase in microvessel permeability (Abstract). *FASEB J* 17: A131, 2003.